

Random Testing to New Limits

George Fox Lang, Independent Consultant, Hatfield, Pennsylvania
Glenn Burroughs, Baker Hughes INTEQ, Houston, Texas
Graham Carmichael, LDS Test and Measurement, Brighton, Michigan

Today's random vibration controllers all facilitate applying limits to the controlled acceleration's power spectral density. Now, alarm and abort limits have been added to the g/volt H -inverse frequency response function at the heart of the control loop and to measured g/g test-object transmissibility. These new limits permit detecting fatigue onset, verifying correct conduct of long-term extreme shakes as well as far better protecting both the device under test and the shaker armature.

LDS Test and Measurement recently introduced a seemingly minor random testing option for its range of Dactron *COMET*_{USB}TM and Dactron *LASER*_{USB}TM vibration controllers. Provision has been made to set Alarm and Abort profiles around g-per-g transmissibility functions between pairs of monitored accelerations or around the volt-per-g H -inverse (H^{-1}) frequency response function (FRF) at the heart of the random control loop. In fact, this small change introduces a profound increase in system utility and capability. Limits of these types, as opposed to the conventional Alarm and Abort profiles applied to controlled and measured g²/Hz power spectral densities (PSD) common to all random controllers, allow automated test shutdown upon the onset of fatigue damage to the device under test (DUT), upon loosening or failure of the mounting fixture or upon structural degradation of the shaker armature guidance and suspension. Read on to discover why one lab director now calls this option his "shaker-protection insurance policy."

Figure 1 illustrates the simple interface dialog for establishing (\pm dB) Alarm and Abort profiles. (For reference, a signal falling outside of the Alarm limits generates a warning message; one exceeding the Abort limits shuts down the shaker and stops the test.) One simply selects the function to be monitored, applies the desired type of limiting and specifies the desired (independent) plus-and-minus tolerances. Both Alarm and Abort limits are always applied to the PSD of the Control signal (shown in the background screen). They may optionally be applied to the PSD of any additional acceleration signal monitored. However, the unique offering presented in Figure 1 is the ability to apply Alarm and/or Abort limits to any measured (g/g) transmissibility between input channels (Figure 1), or the ability to apply them to the (Volt/g) H^{-1} function as shown in Figure 2.

Figure 3 provides a simplistic model of a random vibration testing system. The controller generates an analog Drive signal that is applied to the power amplifier driving the shaker's armature. It varies the spectral shape and root mean square (RMS) of this signal to force the PSD of the Control acceleration to match the user-specified Demand profile PSD. The Control signal is measured by an accelerometer normally mounted on the shaker table or on the nearly rigid base of the DUT firmly attached to the shaker table. Other accelerometers may be mounted on the DUT at sites and in directions of interest. These optional signals are Monitor signals measured by additional controller input channels.

The controller's shaped random generator produces a random time history with a Gaussian amplitude probability distribution function (PDF) and a PSD matching the spectral shape of the desired Demand profile. This signal is equalized for the frequency-dependent gain of the electromechanical subsystem formed by the amplifier, shaker, DUT and mounting structure, the Control accelerometer and all analog signal conditioning circuits. The resulting analog Drive signal is applied to the power amplifier driving the shaker's armature (or hydraulic control valve). The equalization is accomplished using H^{-1} multiplication, where H is a measured FRF reflecting the Control acceleration per volt of Drive signal. The same FFT-based signal processing that guides the evolution of the H^{-1} equalization is used to compute any desired transmissibility FRFs between measured accelerations.

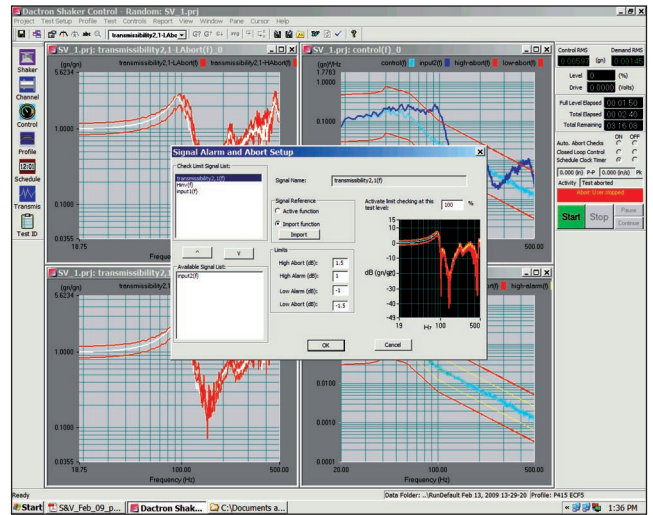


Figure 1. Dactron random control interface showing the Alarm and Abort Setup dialog (with optional capabilities).

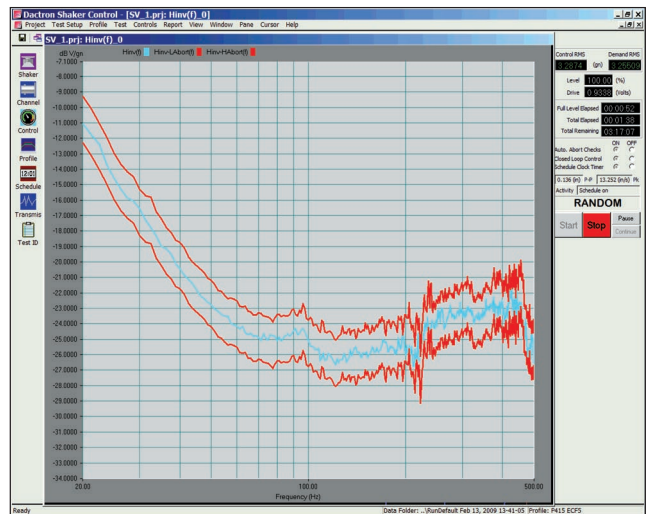


Figure 2. An H -inverse Frequency Response Function shown between programmed Abort limits.

Retiring the Tired – Detecting Fatigue

Figures 4 and 5 present typical displays from a test using transmissibility limits to automatically abort the test. Figure 4 illustrates normal or acceptable operation, while Figure 5 shows the test halted when the transmissibility exceeded an Abort limit. In this example, the purpose of the test was to automatically detect fatigue onset while subjecting the DUT to relatively low-amplitude shaped random excitation. The transmissibility was measured using the shaker table Control signal as a reference (the denominator) and a second accelerometer mounted within the DUT at a location separated from the first by the compliant structural region to be evaluated.

Compare Figures 4 and 5 and note that the Control signal (upper pane) is well within the Alarm limits in both cases. The lower pane transmissibility discloses the reason for the test abort. In Figure 4 the transmissibility is within its Abort limits over the entire 20-500 Hz test bandwidth. In Figure 5, transmissibility may be seen below the lower Abort limit.

Therefore, transmissibility limits automate detection of fatigue onset. This is an important step toward gathering realistic life-

expectancy statistics for the part or assembly being evaluated.

Satanic Simulations Substantiate Strength

Baker Hughes is an international company involved in all aspects of finding, extracting and processing petroleum. Since all of the “easy” sites have been found, oil exploration has become a most scientific business using special-purpose, high-technology equipment. The easily tapped near-surface deposits have all been discovered and are being drained. New oil wells often involve drilling to depths approaching 30,000 feet with down-hole temperatures reaching 300° F; electronic servo drill guidance is mandatory. So Baker Hughes routinely designs and deploys sophisticated acoustic, nuclear, RF resistivity and MRI sensors along with radio-link electronic elements built into a rugged 4.75-in.-diameter “barrel”

housing that follows a 6.75-in. drill bit on its rough and tumble journey literally toward the depths of Hell (see the instrumentation package being deployed in Figure 6).

Operating a drilling rig is very expensive; reliable, test-proven equipment is essential. Baker Hughes INTEQ qualifies all down-hole sensor and electronic packages through a rugged series of environmental simulations. These include a 30-1000 Hz shaped-random shake test at a level of 20 g_{RMS} for 10 hours. Such violent shake tests are expensive. They require a large shaker system run at high power for a long time and retain an expensive piece of custom equipment until the simulation is completed. Learning after the fact that a retaining screw turned loose or part of a fixture gave way during the qualification is totally unacceptable. If any aspect of the DUT mounting fails, the test needs to be terminated immediately,

Statistics of PSD and FRF Measurements

Anyone who has ever measured the frequency response function of a mechanical structure (or electrical filter) using an FFT analyzer and “white” random noise has observed that the FRF measurement “cleans up” much more rapidly than the power spectral density (PSD) of the process’s input and output. That is, the FRF tends to converge to its final shape within a few averages, while the power spectra take many more averages to suppress the random variations masking their central spectral shapes. Classical statistics explain this phenomena, making it clear that FRF rather than PSD limits are the right choice to detect structural changes in a device under test (and/or its mounting) during a random shake test.

A random shake-test basically involves producing and controlling an acceleration signal with a specified PSD spectral shape and a “normal” or Gaussian amplitude distribution. If that acceleration time history is then amplitude squared, the amplitude distribution of the squared signal approaches a different classical statistical distribution called the “Chi-square” (χ^2). Statisticians often characterize such a signal as having “Gaussian mean and Chi-square variance.” Since the power spectral density (PSD) of a signal is the derivative of the variance with respect to frequency, the PSD is also governed by Chi-square statistics.

With a little help from Otnes and Enochson¹ or from Bendat and Piersol,² you can construct the upper and lower bounds of a confidence interval surrounding a PSD’s g²/Hz magnitude. These tolerance extremes define the statistically reasonable maximum scatter of PSD amplitude in your measurement. They allow a statement of the form: “The ratio of my PSD measurement to the true PSD amplitude is no less than A and no more than B at any measured frequency; I can say this with C percent confidence.” Such a statement is formalized by Equation 1.

$$\left(\frac{\chi^2 \left[n, 0.5 + \frac{p}{200} \right]}{n} \right) \leq \frac{\hat{G}_{yy}(f)}{G_{yy}(f)} \leq \left(\frac{\chi^2 \left[n, 0.5 - \frac{p}{200} \right]}{n} \right) \quad (1)$$

where:

$\hat{G}_{yy}(f)$ = measured estimate of PSD from signal y at frequency f

$G_{yy}(f)$ = actual value of PSD from signal y at frequency f
 n = statistical degrees of freedom (DOF) in the averaged $\hat{G}_{yy}(f)$ measurement ($2 \leq n \leq 2N$)

N = number of power spectra ensemble averaged

p = percent confidence in measurement

$\chi^2[n, q]$ = value bounding probability area q under Chi-square curve with n degrees of freedom

The DOF in Equation 1 deserve further discussion. To the first approximation, n corresponds to twice the number of spectra N averaged. This reflects the fact that each unaveraged spectral point reflects *two* independent amplitudes (a real and an imaginary), which are squared and added together to contribute to $\hat{G}_{yy}(f)$. Therefore, each spectrum contributes two DOF to the average, but the relationship between n and N is actually more complex than a simple factor of 2.

In modern controllers, the raw or unaveraged spectra are computed by gathering a block of synchronously sampled contiguous

signal amplitudes and transforming these time-domain samples to a frequency-domain spectrum using the fast-Fourier transform (FFT). As long as each block contains unique information, each spectrum contributes 2 DOF to the averaged power spectrum. (Note that every spectral point in the averaged PSD is a measurement of $2N$ DOF, independent of the block size, sample rate and spectral window weighting function employed.)

However, fast processing systems can compute an FFT in less time than it takes to acquire the time samples required for the spectral transformation. So averaged measurements can easily contain redundant spectra reflecting overlapped time samples. In FFT processing, we acquire data at a constant sample rate and process (transform) the results in constant-sized blocks. When the transform processing is rapid, it can outpace the acquisition so that the input blocks are no longer fully independent of one another. A certain percentage of the sequential time samples are then redundantly processed into adjacent spectral output blocks. The ratio of redundantly processed samples to total time samples defines the processing overlap. Therefore, the relationship between the number of spectra averaged N and the resulting number of DOF may be stated:

$$n = 2 \left[N + \frac{\% \text{ overlap}}{100} (1 - N) \right] \quad (2)$$

The statistically expected scatter in a FRF can also be described by a tolerance interval. However, the form of the bounding equations is quite different, because the FRF is a function of two signals each with Gaussian mean and Chi-square variance. Unlike a PSD, the FRF spectrum is complex-valued, having both a real and an imaginary amplitude (or a magnitude and a phase) at each frequency. Statisticians use the comparative F distribution, a function of two different DOF to form the confidence limits of an FRF. The confidence limits must also consider the linear causality between the input and output signals; this is reflected by the ordinary coherence function $\gamma_{xy}^2(f)$ measured between the two signals.

To model an FRF measured using N tripower spectral averages, the total DOF of the FRF are split into factors 2 and $n-2$. The appropriate F distribution for the desired percent confidence is selected. The ordinary coherence function $\gamma_{xy}^2(f)$ is evaluated, and confidence bounds are formed in accordance with Equation 3:

$$\frac{1}{1 + \sqrt{\frac{2}{n-2} (1 - \gamma_{xy}^2(f)) F[2, (n-2), (p/100)]}} \leq \frac{|\hat{H}_{yy}(f)|}{|H_{yy}(f)|} \leq \frac{1}{1 - \sqrt{\frac{2}{n-2} (1 - \gamma_{xy}^2(f)) F[2, (n-2), (p/100)]}} \quad (3)$$

where:

$|\hat{H}_{xy}(f)|$ = magnitude of measured estimate of FRF-relating signals, x and y , at frequency f

$|H_{xy}(f)|$ = actual magnitude of FRF-relating signals, x and y , at frequency f

since only parts that completely pass all qualifications without question or exception are cleared for field deployment. This is the important function provided by H^{-1} limiting.

Similarly abusive tests are routinely conducted on automotive components. A popular target for such hellish shake tests are throttle bodies, such as those made by KSR International of Ontario, Canada (Figure 7). These devices incorporate feedback sensors including those for tracking throttle-plate angle and oxygen content. Each new design or variation needs to be carefully screened for ruggedness and reliability. This includes a 10-hour random shake using a severe 10-g_{RMS} shaped profile. Again, using H^{-1} Abort limits assures that the device under test “sees” the proper Demand profile for the duration of the test. No part “slips through” with a less intense proof test.

Avoiding Armature Armageddon

Performing a high-g qualification test often requires running the shaker system near its physical limits. This is not a problem as long as the test remains within the planned force, acceleration, velocity and stroke regime. However, anything that happens to change the structural response seen by the Control accelerometer during the test can place the shaker in jeopardy. While blatant failure – such as killing or shedding the accelerometer – will abort the test, more subtle system damage such as an evolving crack in the mounting fixture can spell real trouble.

In Figure 8, an aggressive (15 g_{RMS}) 20-2000 Hz shake is used to qualify another type of automotive sensor made by a different manufacturer. In this test, the Control accelerometer is mounted on the attachment fixture and not on the shaker table. As shown

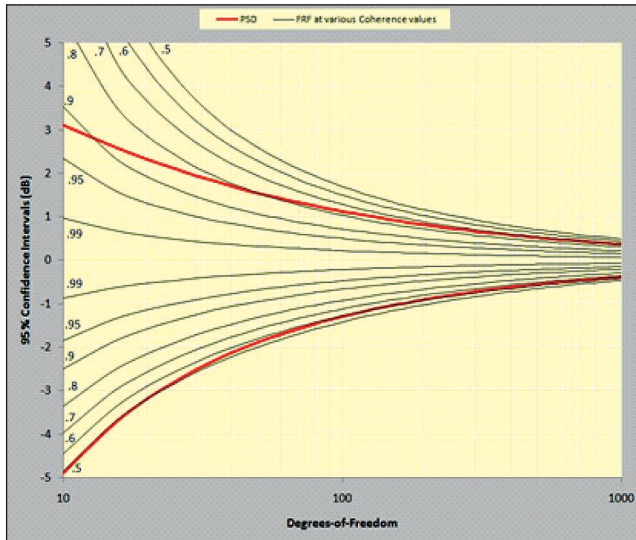


Figure A: 95% confidence limits for PSD (red) and FRF measurements at various coherence (γ^2) values between 0.50 and 0.99.

$$\gamma_{xy}^2(f) = \text{ordinary coherence between signals, } x \text{ and } y, \text{ at frequency } f$$

$$n = \text{statistical DOF in } |\hat{H}_{xy}(f)| \text{ and } \gamma_{xy}^2(f)$$

$$p = \text{percent confidence in measurement}$$

$$F[\alpha, \beta, q] = \text{value bounding probability area } q \text{ under } F \text{ curve relating distributions of } \alpha \text{ and } \beta \text{ DOF}$$

Figure A plots Equations 1 and 3 at 95% confidence. FRF results for Equation 3 are presented at various coherence levels from 0.5 to 0.99. All amplitude ratios have been plotted in dB. The power spectral density confidence limits are calculated as:

$$10 \cdot \log_{10} \left(\frac{\hat{G}_{yy}(f)}{G_{yy}(f)} \right)$$

while the frequency response function confidence limits are computed as:

$$20 \cdot \log_{20} \left(\frac{\hat{H}_{xy}(f)}{H_{xy}(f)} \right)$$

Note that demanding a higher percent confidence “spreads out” the (\pm dB) amplitude confidence limits to more extreme values, while requesting a lower confidence contracts them.

It is clear from these curves that an FRF measurement will converge rapidly if the measured process is linear and the input and output signals are “clean.” That is, if the process coherence is close to 1, only a few spectra need be averaged to provide a good estimate of the true FRF. It is also clear from this figure that a longer averaging time (more DOF) will clean up rather noisy measurements to eventually provide a clear image of the underlying linear relationship.

The dramatic influence of coherence on the relative dispersion of an FRF average compared to a PSD average may be seen clearly by equating the upper and lower bounds of Equations 1 and 3 at

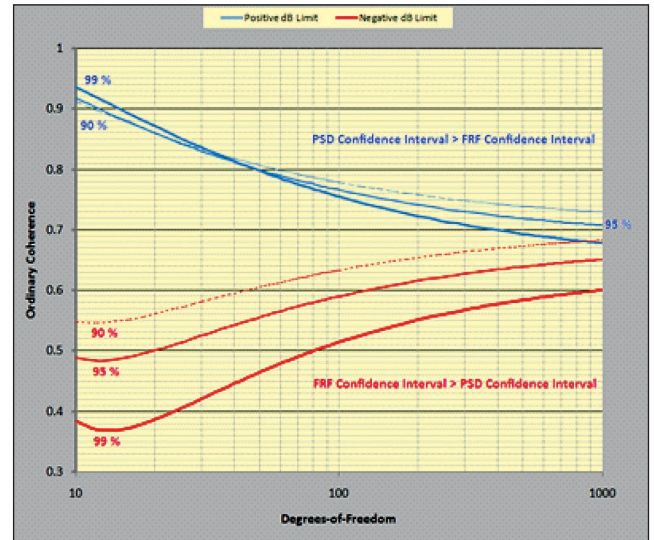


Figure B: Coherence required for equal PSD and FRF tolerance limits versus DOFs for 90%, 95% and 99% confidence.

like DOF and confidence and solving for the coherence (γ^2). Figure B provides these results for 90%, 95% and 99% confidence. This figure illustrates (for example) that at 95% confidence when the tripower averages have 100 DOF, if the coherence is less than 0.590, the FRF has a broader dB tolerance interval than do the associated PSDs. If the coherence exceeds 0.766, the PSDs have broader dB tolerance intervals than the FRF.

This explains why FRF limit testing is more effective than PSD limit testing to detect fatigue damage within the DUT, to detect fixture failures including fasteners that vibrate loose and to guard against ruining your shaker if the armature suspension should suffer degradation. In essence, when the system is tight and healthy, the coherence between Drive and Control signals or between Control and a Monitor channel will be high. Therefore, measured estimates of these FRFs will converge upon their true value much more rapidly than the associated Drive, Control and Monitor PSDs. In part, this explains why H^{-1} based random control works so well. The Volt/g H^{-1} required for control emerges from the noise more rapidly than does the PSD of the acceleration being controlled.

However, when the system being controlled starts to change, the coherence drops off rapidly. This results in an immediate relative increase in the confidence interval for the FRF. That is, the variability of the FRF estimate increases dramatically (compared to the change in variability of the Control signal PSD). Additionally, of course, the control loop continues to work diligently to force the Control signal PSD to match the Demand profile. Therefore, an earlier warning of a system change is provided by limit-testing the transmissibility and H^{-1} FRFs than by testing the system PSDs. While the real-time Alarm and Abort limit testing of the Control PSD remains the first line of equipment defense, the additional FRF tests provide sensitivity to fatigue, cracking and loosening before they reach catastrophic levels and damage the device under test or the shaker.

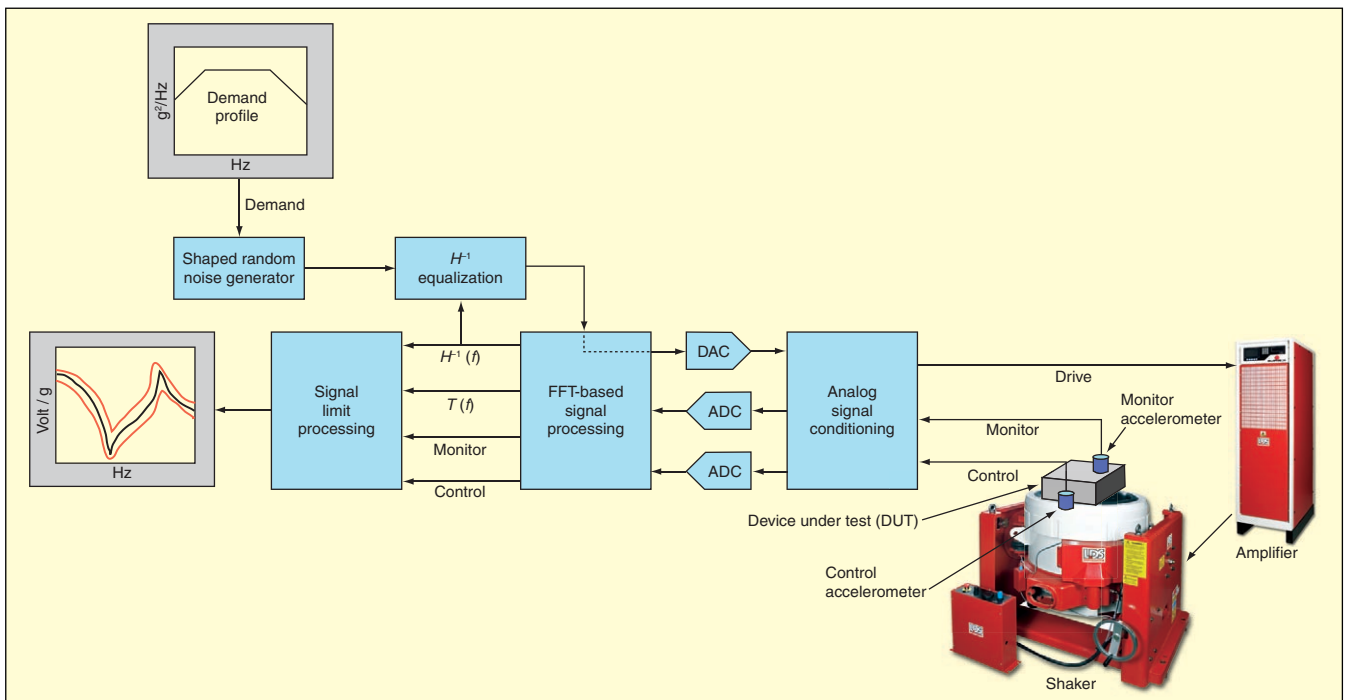


Figure 3: Functional block diagram of a random vibration control system.

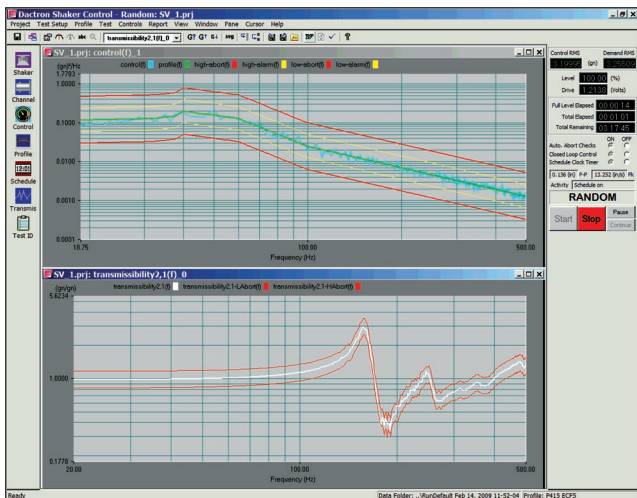


Figure 4. Typical displays from a controlled random test. Upper pane shows Control PSD within Alarm and Abort limits. Lower pane illustrates the Monitor/Control Transmissibility within its own Abort limits.

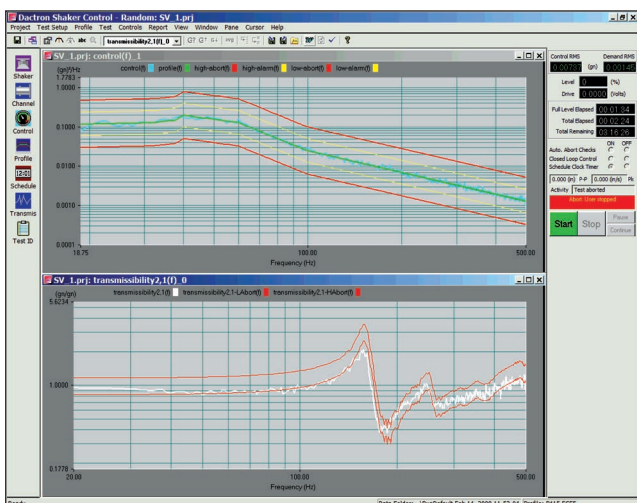


Figure 5. Aborted test displays indicating structural degradation of the DUT. Upper traces show the Control is still within the Alarm limits. Lower trace shows Transmissibility exceeding its Abort limits.

in the lower pane, the Control acceleration is well within specified Alarm and Abort limits. The test is also protected by H^{-1} Abort limits shown within normal expectations (in the upper pane). Compare these results with Figure 9.

In Figure 9, the results of a mounting fixture failure are shown. The Control signal remains well within limits; the test was automatically aborted by the H^{-1} limits. What does *not* show in Figure 9 is the unmonitored shaker table motion required to hold the Control acceleration within limits on the failed fixture. Since the Control accelerometer rode on the upstream side of the fixture damage, it did not reflect the markedly increased downstream table acceleration required to hold control across a cracked fixture. Because this qualification test is deliberately violent, reused fixtures can occasionally fail. This fixture failure caused no shaker damage. One that occurred prior to the use of H^{-1} limiting required a \$43,000 rebuild of the shaker armature with attendant facility down-time.

Observations and Conclusions

As discussed in the accompanying sidebar, FRF-based limit testing tends to respond more rapidly to structural changes than do PSD-based tests. This is especially true when comparing the response of transmissibility or an H^{-1} to a Control signal PSD. After all, your random controller is dutifully trying to hold the Control PSD to a fixed profile. Its control loop is specifically designed to track and compensate for changes in the system's exhibited g/Volt characteristic. Therefore, Control limits serve poorly as DUT damage-onset detectors. In contrast, the controller does nothing to prevent the natural evolution of a transmissibility or H^{-1} as the DUT or its attachment structure changes in strength.

FRF-based limits allow you to design more focused change-detection scenarios. For example, with the Control accelerometer mounted firmly to the shaker table, a change in H^{-1} simply says "something has changed." A change in the modal properties of the DUT will reflect back into H^{-1} . A problem with the shaker's suspension or driving amplifier will also cause a change in the integrity of the mounting fixture and fasteners. All of this "insurance" comes without having to add another sensor or modify the test procedure or apparatus in any way.

Add a second accelerometer mounted to the rigid base of the DUT (above the mounting fixture) and measure its transmissibility to the Control. Now you have a spectral function that is far less sensitive to changes in either the DUT or the shaker, but is quite attentive to consistency of the fixtures and locking fasteners. To gain more sensitivity to the DUT, move the second (monitor) accelerometer



Figure 6: Oil field workers lower test-qualified ruggedized Baker Hughes INTEQ measurement electronics into well shaft.

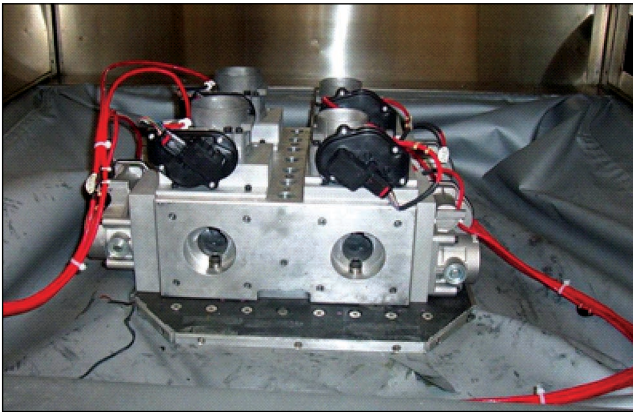


Figure 7: Gang of automotive throttle bodies awaits brutal 10-hour, 10-g_{RMS} shaped-random qualification test.

to a more elastic region of that structure. To focus on a known area of weakness, use the transmissibility between two monitor accelerometers separated by the area in question and oriented in a direction that will experience motion when the target area is stressed. Perhaps most importantly, FRF limiting can save your valuable vibration testing equipment from physical damage.

Being able to apply Alarm and Abort limits to FRFs as well as to PSDs simply makes good sense. It gives the test designer new tools with which to better understand product quality and longevity.

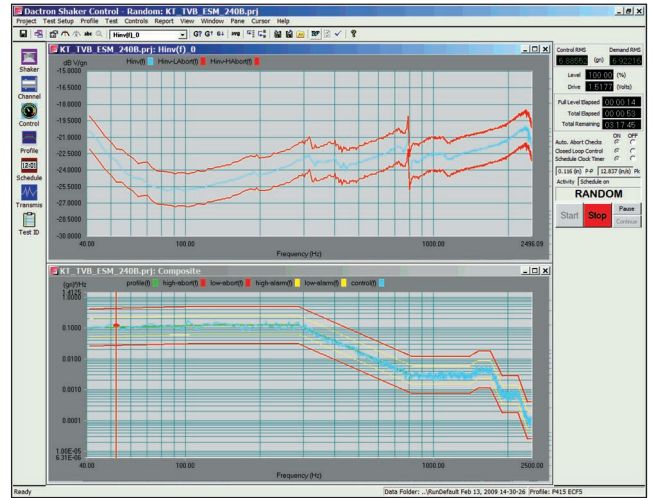


Figure 8. A test running normally; both Control and H^1 are within limits.



Figure 9. The same test automatically shut down by H^1 limits when the fixture failed.

Limits can now be viewed as analytic discriminators, not merely as necessary safeguards. But these additional limits do provide new safeguards, not only for the device being tested, but for the facility equipment employed. Why not routinely employ H^1 limits in combination with multiple transmissibility and PSD limits to fully protect your test and better understand its findings?

References

1. Otnes, Robert K., Enochson, Loren, *Digital Time Series Analysis*, John Wiley & Sons, New York, 1972.
2. Bendat, Julius S., Piersol, Allan G., *Random Data: Analysis and Measurement Procedures*, Wiley-Interscience, New York, 1971. SV

The authors can be reached at: docfox@comcast.net, glenn.burroughs@bakerhughes.com and graham.carmichael@lds.spx.com.